

This Page Is Inserted by IFW Operations  
and is not a part of the Official Record

## BEST AVAILABLE IMAGES

Defective images within this document are accurate representations of the original documents submitted by the applicant.

Defects in the images may include (but are not limited to):

- BLACK BORDERS
- TEXT CUT OFF AT TOP, BOTTOM OR SIDES
- FADED TEXT
- ILLEGIBLE TEXT
- SKEWED/SLANTED IMAGES
- COLORED PHOTOS
- BLACK OR VERY BLACK AND WHITE DARK PHOTOS
- GRAY SCALE DOCUMENTS

**IMAGES ARE BEST AVAILABLE COPY.**

**As rescanning documents *will not* correct images,  
please do not report the images to the  
Image Problem Mailbox.**

**REMARKS**

This amendment is filed in response to the final Office Action dated February 2, 2004. This amendment should be entered, the application allowed, and the case passed to issue.

No new matter or considerations are introduced by this amendment. The amendment to claim 1 is supported in the specification at page 1, line 33 to page 2, line 2, which clearly teaches that the oxygen ion conduction is stronger than electron conduction. The specification discloses that LaGa-based perovskite solid electrodes have an oxygen ion transport number that is about 90 % at 600 °C. The amendments to the specification merely correct informalities.

Claims 1-15 are pending in this application. Claims 6-15 are withdrawn pursuant to a restriction requirement. Claims 1-3 and 5 are rejected. Claim 4 is objected to.

***Objections to the Specification***

The disclosure is objected to because the ion conductivity of Comparative Example b in Table 1 should be 0.018 S/cm, and because brackets allegedly should not be used in the paragraph beginning on line 17 of page 6.

These objections are traversed, and reconsideration and withdrawal thereof respectfully requested. The specification has been amended in accordance with the Examiner's recommendation.

***Claim Rejections Under 35 U.S.C. §§ 102 and 103***

Claims 1, 2 and 5 were rejected under 35 U.S.C. § 102(b) as anticipated by or, in the alternative, under 35 U.S.C. § 103(a) as obvious over Miyashita et al. (U.S. Patent No. 5,731,097).

Claim 3 was rejected under 35 U.S.C. § 103(a) as obvious over Miyashita et al.

These rejections are traversed, and reconsideration and withdrawal thereof respectfully requested. The following is a comparison between the invention as claimed and the cited prior art.

An aspect of the invention, per claim 1, is a solid oxide fuel cell comprising a first perovskite solid electrolyte layer exhibiting mixed conductivity and having oxygen ion conduction which is stronger than electron conduction under operational condition of the solid oxide fuel cell. A fuel electrode is provided on one surface of the first solid electrolyte layer and an air electrode is provided on the opposite side of the first solid electrolyte layer. A second solid electrolyte layer is provided between the first solid electrolyte layer and the air electrode. The second electrode has a lower ratio of conduction by holes and higher ratio of conduction by oxygen ions of the conductive carriers of electrolyte such as ions, electrons, and holes than that of the first solid electrolyte layer under the operational condition of the solid oxide fuel cell.

The Examiner asserted that Miyashita et al. disclose the claimed solid oxide fuel cell comprising an electrolyte layer composed of an LSM film 38 and a YSZ film 36 sandwiched between an anode and cathode. As regards claim 3, the Examiner averred that it would have been obvious to satisfy the formula of claim 3 because the formula depends on the load current density that the fuel cell is subjected to and the given values for the first electrolyte layer thickness and the second electrolyte layer thickness and the load current density of the solid oxide fuel cell varies depending on the load demand and the maximum load current density that J can have is an inherent value of the solid oxide fuel cell.

Miyashita et al. do not anticipate or suggest the claimed solid oxide fuel cell.

Miyashita et al. disclose a solid oxide fuel cell consisting of “cathode / YSZ / LSM / anode” in column 6, lines 23-48. While, LSM is a perovskite solid electrolyte material with mixed conductivity, LSM has an electron conduction which is inherently much stronger than oxygen ion conduction under operational condition of the SOFC, therefore the oxygen ion transport number of LSM is very low. Generally, a solid electrolyte is required to transport oxygen ions. While LSM can be employed as an air electrode, it is not suitable for use as a solid electrolyte material because of its low oxygen ion transport number. The low oxygen ion transport of LSM is disclosed in Khanlou et al., *Electrochemical And Microstructural Study Of SOFC Cathodes Based On La<sub>0.65</sub>Sr<sub>0.3</sub>MnO<sub>3</sub>* (Appendix A), which teaches the electric property of LSM (La<sub>0.65</sub>Sr<sub>0.3</sub>MnO<sub>3</sub>). As disclosed in Fig. 2 on page 479, the total electrical conductivity of (σ<sub>e</sub>) of LSM, which includes oxygen ion conduction and electron conduction, is 200 to 220 S/cm at 600 to 800 °C. The ionic conductivity of LSM (σ<sub>i</sub>), which corresponds to oxygen ion conduction, is 2 × 10<sup>-4</sup> to 4 × 10<sup>-4</sup> S/cm at 850 to 1000 °C. According to the data disclosed by Khanlou et al., the oxygen ion conduction of LSM is much weaker than electron conduction of LSM under operational conditions of a solid oxide fuel cell. The LSM layer is clearly distinguishable from the first perovskite solid electrolyte layer required by claim 1. Miyashita et al. do not disclose a solid electrolyte layer exhibiting mixed conductivity and having oxygen ion conduction which is stronger than electron conduction under operational condition of the solid oxide fuel cell, as required by claim 1.

The factual determination of lack of novelty under 35 U.S.C. § 102 requires the disclosure in a single reference of each element of a claimed invention. *Helifix Ltd. v. Blok-Lok Ltd.*, 208 F.3d 1339, 54 USPQ2d 1299 (Fed. Cir. 2000); *Electro Medical Systems S.A. v. Cooper Life Sciences, Inc.*, 34 F.3d 1048, 32 USPQ2d 1017 (Fed. Cir. 1994); *Hoover Group, Inc. v. Custom Metalcraft, Inc.*, 66 F.3d 399, 36 USPQ2d 1101 (Fed. Cir. 1995); *Minnesota Mining & Manufacturing Co. v. Johnson & Johnson Orthopaedics, Inc.*, 976 F.2d 1559, 24 USPQ2d 1321 (Fed. Cir. 1992); *Verdegaal Bros. v. Union Oil Co. of California*, 814 F.2d 628, 631, 2 USPQ2d 1051 (Fed. Cir. 1987). Because Miyashita et al. do not disclose the perovskite electrolyte layer having oxygen ion conduction which is stronger than electron conduction under operation condition of the solid oxide fuel cell, as required by claim 1, Miyashita et al. do not anticipate claim 1.

Applicants further submit that Miyashita et al. do not suggest the claimed solid oxide fuel cell with the claimed perovskite solid electrolyte layer and the oxygen ion conductivity.

Obviousness can only be established by combining or modifying the teachings of the prior art to produce the claimed invention where there is some teaching, suggestion, or motivation to do so found either explicitly or implicitly in the references themselves or in the knowledge readily available to one of ordinary skill in the art. *In re Kotzab*, 217 F.3d 1365, 1370 55 USPQ2d 1313, 1317 (Fed. Cir. 2000); *In re Fine*, 837 F.2d 1071, 5 USPQ2d 1596 (Fed. Cir. 1988); *In re Jones*, 958 F.2d 347, 21 USPQ2d 1941 (Fed. Cir. 1992). There is no suggestion in Miyashita et al. to modify the solid oxide fuel cell so that it has a perovskite electrolyte layer having oxygen ion conduction which is stronger

than electron conduction under operation condition of the solid oxide fuel cell, as required by claim 1.

The requisite motivation to support the ultimate legal conclusion of obviousness under 35 U.S.C. § 103 is not an abstract concept, but must stem from the applied prior art as a whole and realistically impel one having ordinary skill in the art to modify a specific reference in a specific manner to arrive at a specifically claimed invention. *In re Deuel*, 51 F.3d 1552, 34 USPQ2d 1210 (Fed. Cir. 1995); *In re Newell*, 891 F.2d 899, 13 USPQ2d 1248 (Fed. Cir. 1989). Accordingly, the Examiner is charged with the initial burden of identifying a source in the applied prior art for the requisite realistic motivation. *Smiths Industries Medical System v. Vital Signs, Inc.*, 183 F.3d 1347, 51 USPQ2d 1415 (Fed. Cir. 1999); *In re Mayne*, 104 F.3d 1339, 41 USPQ2d 1449 (Fed. Cir. 1997). There is no motivation in Miyashita et al. to modify the fuel cell so that it has a perovskite electrolyte layer having oxygen ion conduction which is stronger than electron conduction under operation condition of the solid oxide fuel cell, as required by claim 1.

The only teaching of the solid oxide fuel cell with the claimed first perovskite solid electrolyte layer having oxygen ion conduction which is stronger than electron conduction under operation condition of the solid oxide fuel cell is found in Applicants' disclosure. However, the teaching or suggestion to make a claimed combination and the reasonable expectation of success must both be found in the prior art, and not based on applicant's disclosure. *In re Vaeck*, 947 F.2d 488, 20 USPQ2d 1438 (Fed. Cir. 1991). The motivation for modifying the prior art must come from the prior art and must be based on facts.

As regards claim 3, Applicants submit that claim 3 is allowable for at least the same reasons as claim 1.

The dependent claims are further distinguishable over the cited references. For example, claim 2 further requires that the oxygen ion conductivity, oxygen ion transport number and a thickness of the first solid electrolyte layer are respectively  $\sigma_p$ ,  $t_{po}$  and  $L_p$ ; oxygen ion conductivity, oxygen ion transport number and a thickness of the second solid electrolyte layer are respectively  $\sigma_c$ ,  $t_{co}$  and  $L_c$ ; and the following formula is satisfied:  $L_p/(t_{po} \cdot \sigma_p) > L_c/(t_{co} \cdot \sigma_c)$ . Claim 5 further requires that the second solid electrolyte layer is made of stabilized zirconia, or alternatively a ceria based oxide. The cited references do not suggest the claimed solid oxide fuel cell with these additional limitations.

***Allowable Subject Matter***

Claim 4 is objected to as being dependent upon a rejected base claim, but would be allowable if rewritten in independent form. Applicants gratefully acknowledge the indication of allowable subject matter. However, because Applicants believe that independent claim 1 is allowable for the reasons explained above, Applicants do not believe it is necessary to rewrite claim 4 in independent form.

In light of the Remarks above, this amendment should be entered, the application allowed and the case passed to issue. If there are any questions regarding this Amendment or the application in general, a telephone call to the undersigned would be appreciated to expedite the prosecution of the application.

To the extent necessary, a petition for an extension of time under 37 C.F.R. 1.136 is hereby made. Please charge any shortage in fees due in connection with the filing of this

**09/897,116**

paper, including extension of time fees, to Deposit Account 500417 and please credit any excess fees to such deposit account.

Respectfully submitted,

MCDERMOTT, WILL & EMERY



Bernard P. Codd

Registration No. 46,429

600 13<sup>th</sup> Street, N.W.  
Washington, DC 20005-3096  
(202) 756-8000 BPC:BPC  
Facsimile: (202) 756-8087  
**Date: April 30, 2004**

09/897, 1/16

## ELECTROCHEMICAL AND MICROSTRUCTURAL STUDY OF SOFC CATHODES BASED ON $\text{La}_{0.85}\text{Sr}_{0.13}\text{MnO}_3$ AND $\text{Pr}_{0.8}\text{Sr}_{0.1}\text{MnO}_3$

Ariane Ahmad-Khanlou, Frank Tietz, Izak C. Vinke, Detlev Stöver

Forschungszentrum Jülich

Institut für Werkstoffe und Verfahren der Energietechnik,  
D-52425 Jülich, Germany

### ABSTRACT

In order to verify the influence of electrical transport properties of selected perovskites on fuel cell performance, the compounds  $\text{Pr}_{0.8}\text{Sr}_{0.1}\text{MnO}_3$  and  $\text{La}_{0.85}\text{Sr}_{0.13}\text{MnO}_3$  were investigated as cathode materials in single cell tests. The sintering temperatures of the cathode layers were varied between 1100°C and 1250°C to investigate the influence of the microstructure of the cathode coatings on fuel cell performance. The cathode layers sintered at low temperature exhibited microstructures with sub- $\mu\text{m}$  fine grains. According to the electrochemical data, highest cell performances were achieved for both compositions after sintering at 1100°C. In cases where the mixed ionic-electronic conductivity differs by less than one order of magnitude for the materials considered, the material properties play only a minor role in comparison to the microstructural properties.

### INTRODUCTION

With a view to lowering the operating temperature of Solid Oxide Fuel Cells (SOFC) without significant performance losses, the cathode is one of the most critical components. Its properties such as electrical conductivity and oxygen reduction kinetics at the cathode-electrolyte interface play a significant role in determining SOFC performance. Therefore many efforts have been made world-wide to develop alternative, more electrocatalytically active cathode materials to increase the power densities of the cells.

Furthermore, chemical interactions and aging effects are arguments for the reduction of the SOFC operating temperature from approx. 850°C to lower temperatures, in order to improve the long-term stability of the SOFC. However, when the operating temperature drops, there is a substantial increase in the cathodic overvoltage of the state-of-the-art cathode material based on lanthanum manganite. Therefore a cathode with better electrocatalytic properties is needed. Cathode materials containing iron and cobalt are preferred in the literature because of their excellent transport and catalytic characteristics (1,2). However, their tendency to interact with the state-of-the-art electrolyte material, yttria-stabilized zirconia (YSZ), is a problem (3). A few investigations revealed that an improvement of the electrocatalytic activity can be obtained by the variation of the lanthanide element (4). In particular, it is reported that praseodymium exerts a positive influence on the overpotential (5). Perovskites with the

general formula  $\text{A}_{1-x}\text{BO}_3$  are favorable candidates due to their low tendency to form insulating reaction layers with YSZ (6-8). They also exhibit a higher ionic conductivity due to the additional oxygen vacancies in the perovskite lattice which lead to higher cell performances than the stoichiometric perovskites (9-12). Several investigations focused on mixed conducting cathode materials and have shown that such materials are desirable and favorable in order to increase the power density of fuel cells (13-15). Therefore the application of perovskite cathodes on the basis of  $\text{La}_{0.85}\text{Sr}_{0.13}\text{MnO}_3$  with  $\text{Ln} = \text{La}$  and  $\text{Pr}$  was examined in a comparative study by electrochemical measurements on single cells.

The aim of this work was to investigate and verify a) the influence of transport properties and b) the influence of the cathode microstructure on the cell performance by varying the sintering temperature of the cathode layers between 1100°C and 1250°C. By changing the microstructure, the number of three-phase boundaries (TPBs), i.e. the interfaces where cathode, electrolyte and pore meet, changes as well which has a direct influence on cell performance since the electrochemical reaction takes place here (16,17).

### EXPERIMENTAL

The starting materials  $\text{La}_{0.85}\text{Sr}_{0.13}\text{MnO}_3$  (LSM) and  $\text{Pr}_{0.8}\text{Sr}_{0.1}\text{MnO}_3$  (PSM) were spray-dried powders, prepared from nitrate salts (18), calcined at 900°C for 3 hours and milled for several hours to reach a specific grain size. For electrical conductivity measurements the milled powders were pressed uniaxially with 250 MPa and subsequently sintered at 1300°C in air for 10 hours. The total conductivity was measured by four-probe dc measurements on sintered rods (25  $\times$  3  $\times$  3 mm<sup>3</sup>) between 25 and 900°C in air. The ionic conductivity of the two compounds was investigated by permeation measurements without applying an electric field. The two surfaces of dense sintered pellets were exposed to gas flows with different oxygen partial pressure (air and argon). The permeation flux of oxygen from the high- to the low-pressure side was measured using the solid electrolyte technique (19). At each temperature (between 700°C and 1000°C) an equilibrium time was required before the permeation flux was measured. The permeability measurements made within this work can be regarded as a conductivity measurement in an oxygen potential gradient. Instead of applying a voltage, a difference in chemical potential of oxygen is applied and the oxygen ion transport is measured by the ionic current. Therefore, the ionic conductivity measurements in an oxygen potential gradient (19) is the sum of exchange kinetics and the bulk ion diffusion. If the ionic conductivity is rate limiting then the exchange kinetics is better than the measured flux of oxygen ions. On the contrary, the ionic conductivity is underestimated if the oxygen exchange kinetics are rate limiting. However, the knowledge of the rate limiting step is not necessarily essential for application, but high conductivity and good exchange kinetics are required and the sum of both can be evaluated by the permeability measurements. Experimental arrangements and theoretical details are reported in (19-21).

The cells (50  $\times$  50 mm<sup>2</sup>) for electrochemical characterization were manufactured according to previously reported processing steps (22). Both LSM and PSM powders were subjected to a uniform preparation process in order to guarantee comparable layers and to achieve a similar grain-size distribution. The thickness of the SOFC components are 15  $\mu\text{m}$  for the electrolyte (yttria-stabilized zirconia, YSZ), 1500  $\mu\text{m}$  for the anode and anode substrate (Ni/YSZ cermet) and 50  $\mu\text{m}$  for the cathode as reported previously (23).

09/897, 1/16

The cathode is composed of two layers, a composite layer made of cathode material and YSZ (60:40 wt-%) and a layer containing pure cathode material. The cathode layers were applied onto the sintered electrolyte by means of wet powder spraying (WPS<sup>®</sup>) (22) and sintered at 1100°C, 1150°C, 1200°C and 1250°C for 3 hours in air.

For the current-voltage measurements (I-U measurements), the cells were placed in an aluminum housing in which channels were machined for the gas supply. For current collection, a platinum mesh was used on the cathode side and a nickel mesh on the anode side. A gold ring was used to seal the gas compartments. The cells were heated in the furnace and the anode was reduced slowly at 900°C. During the I-U measurements air was supplied to the cell on the cathode side, a fuel gas composed of H<sub>2</sub> with 1.4% H<sub>2</sub>O was supplied to the cell on the anode side. Fig. 1 shows a typical measurement sequence, where temperature, voltage and current are plotted against time. The I-U characteristics were measured galvanostatically in the temperature range between 650°C and 900°C. To investigate the aging effect on the power density two series of I-U measurements were performed before (1<sup>st</sup> measurement) and after the cells were kept at 800°C and a load of 0.3 A/cm<sup>2</sup> for approx. 100 h (2<sup>nd</sup> measurement).

The subject of the electrochemical investigations in this work is to record the dependence of power densities of the various cathodes under working conditions on different cathode materials and microstructures. To prove the reproducibility of the power outputs, at least two identically cells were produced and electrochemically characterized. As long as composition and microstructure of electrolyte and anode of all cells are comparable, the resulting changes in the cell performances correspond to the properties of the cathode layers.

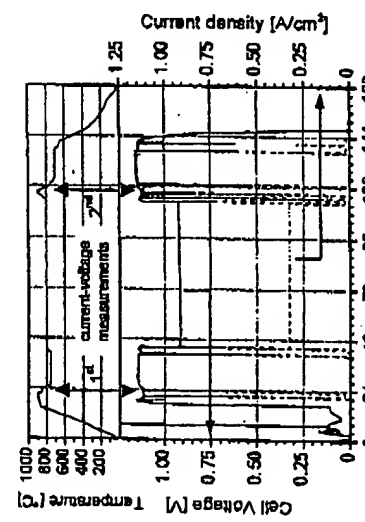


Fig. 1: Measurement sequence for the electrochemical test of single cells. Here the measurement of a cell with PSM cathode sintered at 1100°C is shown.

For the subsequent microstructural investigations of the cells, fracture surfaces of the cathode layers were examined in a scanning electron microscope (JEOL, JSM T 300). Quantitative image analysis was performed on polished samples in order to determine the particle sizes and the porosity of the composite cathode layer. Objects or phases can be

detected and separated from their matrix on the basis of their gray-scale values (24). The area fraction of porosity and solid phases as well as the mean intercept length of the particles and pores in the cathode layers were analyzed with the KS400 software package (Kontron Electronics GmbH) and evaluated as described in (24) and (25).

## RESULTS AND DISCUSSION

The measurements of the electrical and ionic transport properties of LSM and PSM (Fig. 2) revealed that the substitution of La by Pr causes on the one hand a slight decrease of the electrical total conductivity ( $\sigma_e$ ), but on the other hand an increase of the ionic conductivity ( $\sigma_i$ ) by a factor of approx. 3.5. For both perovskites the electronic conductivity is regarded as sufficient for application in SOFCs, better cell performance was expected in the case of PSM as cathode material, because of its superior ionic conductivity.

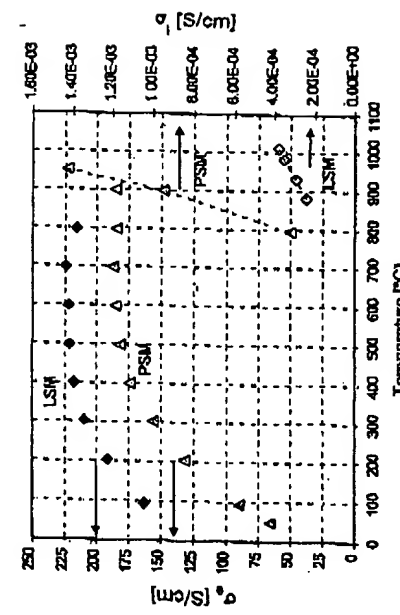


Fig. 2: Total ( $\sigma_e$ ) and ionic ( $\sigma_i$ ) conductivity of LSM and PSM.

The power densities for cells with both types of cathode materials are shown in Fig. 3 for different sintering temperatures and as a function of operating temperature. In this figure the values of the second I-U measurements after several days at constant load were used as shown in Fig. 1. In general the power output decreases with increasing sintering temperatures. Only at low operating temperatures do PSM-containing cells show a slight increase in cell performance. Moreover, the LSM cathode performs better at higher operating temperatures even if the ionic conductivity of PSM is more than three times higher at temperatures above 850°C (Fig. 2). Investigations on the microstructure were consulted to interpret the observed power densities.

The fracture surface of LSM and PSM cathode layers of single cells sintered at different temperatures and after operation are shown in Figs. 4a to 4f. The microstructure of both cathodic layers becomes considerably coarser with increasing sintering temperatures. The finest microstructure was observed for the series sintered at 1100°C

09/897/116

(Figs. 4a and 4d). The particles have already formed sintered necks and are well connected to each other. Due to the higher porosity the active surface area is increased (i.e. increase of TPBs). An increase of the sintering temperature of 50°C results in a coarser microstructure which leads to a decrease in porosity and therefore a smaller number of TPBs (Figs. 4b and 4e). After sintering at 1200°C the particles form agglomerates which result in a stronger reduction of the TPBs and the porosity. For further interpretation of the electrochemical data it should be taken into account that the pure cathode layer (C-layer) in the LSM-containing cell (Fig. 4c) shows a higher porosity compared to PSM (Fig. 4f). The highest density of the layers was obtained after heat treatment at 1250°C, hardly any pore channels were detectable, therefore this sintering temperature is not suitable for cathode fabrication.

The I-U-characteristics of the cells and the investigations on the microstructure of the cathode layers revealed that the microstructure plays a more significant role in the power output than the choice of the lanthanide ion. The material properties show less influence on the resulting power densities than expected. The lowest power density was found for cells sintered at 1250°C. Due to the densification of the cathode layer a) the amount of TPB is significantly reduced and b) ineffective pore channels are formed for gas transport which might lead to low power densities due to insufficient gas diffusion. However, due to the low fuel utilization during the current-voltage measurements diffusion limitation could not be observed. With decreasing sintering temperature, the particles in the layer coarsen to a smaller extent, so that a finer microstructure is observed, that leads to higher porosity and higher number of TPBs. But not only the microstructure of the catalytic active layer is of importance. In the case of sintering at 1200°C, the power output of the LSM-containing cell is higher than the PSM cell, although the composite layers of both cells had a similar microstructure and showed both intergranular fracture surfaces (Figs. 4c and 4f, CC-layers). This observation can be explained by the higher density of the pure cathode layer of the PSM cell (Fig. 4f, C-layer). The C-layer of the PSM cell is much denser impeding the oxygen flux towards the TPBs. Therefore, the LSM-containing cell sintered at 1200°C shows somewhat higher cell performance.

In order to verify the changes in the microstructure with sintering temperature, the mean intercept length of the particles in the composite layer (i.e. the sum of perovskite and YSZ grain sizes) and the porosity of the layers were measured by quantitative image analysis. In this case it was not sufficiently possible in SEM back-scattering mode to distinguish between perovskite and YSZ particles due to their recognizable but digitally not well resolvable gray-scale values. However, from the optical impression of the back-scattering images it is a good estimation for the particle sizes of the single phases to take half of the measured intercept lengths. Fig. 5 shows a correlation of the power densities of the LSM- and PSM-containing cells with the mean intercept length of the particles for two I-U measurements at different temperatures. The best performance was observed for cathode layers sintered at 1100°C, which show that besides a fine microstructure a sufficient high porosity (approx. 31%) is necessary to reach best cell performances. With increasing sintering temperature, the particles sinter to denser agglomerates and the amount of TPBs is decreased. The porosity obtained after sintering at 1150°C was approx. 29% for both CC-layers. In the case of cathodes sintered at 1200°C, a stronger agglomeration of particles in the CC-microstructure was obtained (porosity of approx. 22%). The power output is additionally affected by the different microstructures of the pure cathode layer (Figs. 4c and 4f, C-layer) as mentioned before. The porosity of the composite cathode

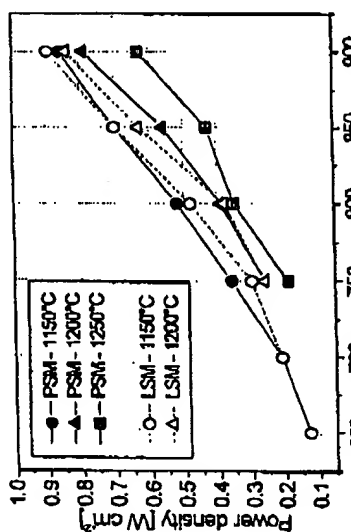


Fig. 3: Power densities of cells containing PSM or LSM as cathode for different sintering temperatures as a function of operating temperature.

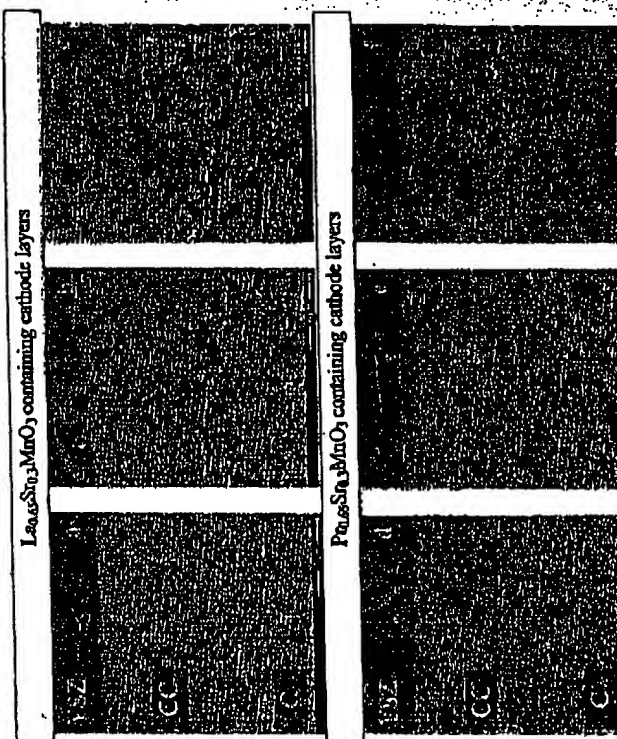


Fig. 4: Fracture surface of LSM (top) and PSM (bottom) cathodes in single cells after operation, C: cathode layer, OC: composite cathode layer (YSZ and cathode material), a) and d) sintered at 1100°C, b) and e) sintered at 1150°C, c) and f) sintered at 1200°C each for 3 h.

09/8977/14

layer sintered at 1250°C was less than 6%, which was far too low to guarantee sufficient gas transport for high cell performance.

Thus series of investigations clearly indicates that the reduction in sintering temperature from currently 1200°C to 1100°C should be favorable from several points of view: it results in an increase in the amount of the TPBs, there is an increase in porosity for the gas supply and the possibility of chemical interaction between the cathode and the electrolyte is reduced. Furthermore, it was established that PSM can be used as an alternative, slightly more electrocatalytic effective cathode material which led to slightly higher power densities for temperatures  $\leq 800^\circ\text{C}$  as long as the microstructure is optimized.

## ACKNOWLEDGMENTS

The authors thank Prof. H. Ultman (Dresden University of Technology, Germany) and Dr. N. Trofimenko (Fraunhofer Gesellschaft-IKTS Dresden, Germany) for the measurements of the ionic conductivity

## REFERENCES

- (1) B. C. Steele, *Solid State Ionics*, 86-88, 1223 (1996).
- (2) J. A. Lauer, S. J. Benson, D. Waller, J. A. Kilkis, *Solid State Ionics*, 121, 201 (1999).
- (3) C. C. Chen, M. M. Nasrallah, H. U. Andersson, in *Solid Oxide Fuel Cells III*, S. C. Singhal and H. Iwahara, Editors, PV 93-4, p. 598, The Electrochemical Society Proceedings Series, Pennington, NJ (1993).
- (4) Y. Terada, T. Nobunaga, K. Okamoto, N. Miura, N. Yamane, *Solid State Ionics*, 48, 207 (1991).
- (5) T. Ishihara, T. Kubo, H. Matsuda, Y. Tabata, *J. Electrochem. Soc.*, 142, 1519 (1995).
- (6) H. Yokohawa, N. Sakai, T. Kawada, M. Dokuya, in *Solid Oxide Fuel Cells I*, S. C. Singhal, Editor, PV 89-11, p. 118, The Electrochemical Society Proceedings Series, Pennington, NY (1989).
- (7) B. Ghatage, T. Peiguer, A. Hammou, in *Rise 14<sup>th</sup> Int. Symp. Material Science*, F. W. Poulsen, J. J. Bentzen, T. Jacobsen, E. Skou and M. J. L. Østergaard, Editors, p. 249, Deauvoir, (1999).
- (8) G. Sachtler, E. Sjöström, A. Naoumidis, *J. Am. Ceram. Soc.*, 73, 929 (1990).
- (9) X. Huang, J. Liu, Z. Li, W. Liu, L. Pei, T. He, *Z. Liu, W. Su, Solid State Ionics*, 130, 195 (2000).
- (10) O. Yamamoto, Y. Takeeda, T. Kojima, in *Solid Oxide Fuel Cells I*, S. C. Singhal, Editor, PV 89-11, p. 148, The Electrochemical Society Proceedings Series, Pennington, NJ (1989).
- (11) J. W. Stevenson, T. R. Armstrong, W. J. Weber, in *Solid Oxide Fuel Cells IV*, M. Dokuya, O. Yamamoto, H. Tagawa and S. C. Singhal, Editors, PV 95-1, p. 454, The Electrochemical Society Proceedings Series, Pennington, NJ (1995).
- (12) J. Mizusaki, H. Nambu, C. Nakao, H. Tagawa, H. Minamide, T. Hashimoto, in *Solid Oxide Fuel Cells IV*, M. Dokuya, O. Yamamoto, H. Tagawa and S. C. Singhal, Editors, PV 95-1, p. 444, The Electrochemical Society Proceedings Series, Pennington, NJ (1995).
- (13) H. H. Möbius, *Wiss Zeitschrift der Universität Rostock* 18, 935 (1969).
- (14) M. Mogensen, in *Rise 14<sup>th</sup> Int. Symp. Material Science*, F. W. Poulsen, J. J. Bentzen, T. Jacobsen, E. Skou and M. J. L. Østergaard, Editors, p. 117, Denmark (1993).
- (15) J. A. Kilkis, in *Ionic and Mixed Conducting Ceramics II*, T. Ramaswamy, W. Worrell and H. L. Miller, Editors, p. 174, Electrochemical Society, New Jersey (1994).
- (16) T. Inoue, K. Eguchi, T. Setoguchi, H. Arai, *Solid State Ionics*, 48/41, 407 (1990).
- (17) K. Sakai, J.-P. Wirth, R. Gschwend, M. Gödickemeier, L.J. Gauckler, *J. Electrochim. Soc.*, 143, 530 (1996).

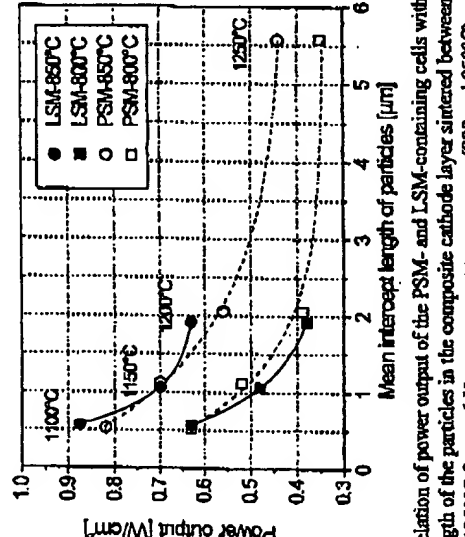


Fig. 5. Correlation of power output of the PSM- and LSM-containing cells with the mean intercept length of the particles in the composite cathode layer sintered between 1100 and 1250°C for two I-U measurement temperatures (800 and 850°C).

## CONCLUSIONS

The possible application of an alternative perovskite with the composition  $\text{Pr}_{0.8}\text{Sr}_{0.1}\text{MnO}_3$  as cathode material in SOFC was examined by measuring the electrochemical performance on  $5 \times 5 \text{ cm}^2$  single cells in comparison to the performance of cells containing LSM cathodes. Sintering experiments served to evaluate the conditions for the thermal treatment of the PSM and LSM cathode coatings. A reduction in the sintering temperature of the cathode layers from currently 1200°C to 1100°C has the advantage of a more efficient system which also exhibits less chemical interaction. PSM showed only a slight increase in ionic conductivity compared to LSM. In cases where the ionic conductivity differs by less than one order of magnitude, the material properties play only a minor role in comparison to microstructural parameters.

09/897, 11/6

- (18) P. Kountouras, R. Färthmann, A. Naoumidis, G. Stachnol, E. Syrakis, *Ionics*, 1, 40 (1995).
- (19) J. M. Paulsen, in *Thermodynamic, oxygen stoichiometric effects and transport properties of ceramic materials in the system Sr-Ce-M-O (M=Co, Fe)*, PhD-Thesis Dresden University of Technology, Germany, (1997).
- (20) H. Ullmann, J. Paulsen, N. Trofimko, in *Rise 17th Int. Symp. Material Science*, F. W. Poulsen, N. Boenzen, S. Linderoth, M. Mogensen, B. Zachau-Christiansen, Editors, p.455, Denmark (1996).
- (21) H. Ullmann, N. Trofimko, F. Tietz, D. Striver, A. Ahmed-Khanian, *Solid State Ionics*, 138, 79 (2000).
- (22) H. P. Buckkemper, U. Diekmann, D. Striver, in *European SOFC Forum II*, B Thorstensen, Editor, p. 221 (1996).
- (23) D. Striver, U. Diekmann, U. Fleisch, H. Kabs, W. J. Quadakkers, F. Tietz, I. C. Vinke, in *Solid Oxide Fuel Cells 1/2*, S. C. Singhal and M. Dokya, Editors, PV 99-19, p. 812, The Electrochemical Society Proceedings Series, Pennington, NJ (1999).
- (24) D. Stanwix, F. Tietz, D. Striver, *Solid State Ionics*, 132, 241 (2000).
- (25) E. E. Underwood, in *Metals Handbook 9th Edition, Vol. 9 Metallography and Microstructure: Quantitative Metallography*, K. Mills, J. R. Davis, J. D. Deschka, D. A. Dietrich, G. M. Crandall, H. J. Frissell and D. M. Jenkins, Editors, p. 123, American Society for Metals, Ohio, (1985).

## IMPROVED PERFORMANCE OF $\text{La}_{0.8}\text{Sr}_{0.2}\text{MnO}_3$ CATHODES BY SOL-GEL COATINGS

Sung Pil Yoon, Suk Woo Nam, Tae-Hoon Lim, Jonghee Han, Seong-Ata Hong  
Battery and Fuel Cell Research Center,  
Korea Institute of Science and Technology (KIST)  
Hawolgok-Dong 39-1, Seongbuk-Gu, Seoul 136-791, Korea

### ABSTRACT

Sol-gel coating technique has been applied to deposit films of yttria-stabilized zirconia (YSZ) or samaria-doped ceria (SDC) within the pores of  $\text{La}_{0.8}\text{Sr}_{0.2}\text{MnO}_3$  (LSM) cathodes. The composite cathodes have potential advantages as the new electrode has stable and individual paths for electrons and ions due to the formation of YSZ or SDC filaments between electrode/electrolyte interface at low sintering temperature ( $< 800^\circ\text{C}$ ). For the LSM cathodes modified by sol-gel coating, percolation problems and resistive compounds, such as  $\text{La}_2\text{Zr}_2\text{O}_7$  and  $\text{SrZrO}_3$ , were not observed. The  $R_p$  of the LSM cathode modified with SDC sol was only  $0.12 \Omega\text{cm}^2$  at  $750^\circ\text{C}$  and air atmosphere. The result implied that deposition of YSZ or SDC in the pore surface of cathode increased the area of triple phase boundary between air, LSM cathode and YSZ electrolytes, resulting in the improved cathode performance for applications in reduced-temperature solid oxide fuel cells.

### INTRODUCTION

Conventional solid oxide fuel cells (SOFCs) are operated around  $1000^\circ\text{C}$ . Such a high operating temperature of SOFCs can lead to several problems, which include electrode sintering, interfacial diffusion between electrolyte and electrode materials, and mechanical stress due to different thermal expansion coefficients (TEC) of the cell components (1). Thus, lowering the operating temperature is desirable for overcoming such problems. Moreover, at an operating temperature down to around  $700^\circ\text{C}$ , a low-cost ferritic steel interconnector can be used. However, the low operating temperature decreases the cell performance because of the low ionic conductivity of yttria-stabilized zirconia (YSZ) and the high over-potential of electrodes, especially at the cathode side. Recently, many efforts have been devoted to reduce Ohmic losses and electrode polarization ( $R_p$ ) for the low operating temperature (2-3). For example, mixed electronic and ionic conductors (MEC) such as  $\text{La}_{0.8}\text{Sr}_{0.2}\text{Fe}_{0.7}\text{Co}_{0.3}\text{O}_3$  have been studied as alternative cathode material because it has a higher ionic conductivity than the other perovskites. But it has poor compatibility with YSZ electrolyte in terms of formation of  $\text{La}_2\text{Zr}_2\text{O}_7$  or  $\text{SrZrO}_3$  and mis-match of TEC.

In view of the adequate compatibility with YSZ electrolyte,  $\text{La}_{0.8}\text{Sr}_{0.2}\text{MnO}_3$  is most commonly used as a cathode material for SOFCs. Under normal SOFC operating condition, however, LSM exhibits nearly 100% electronic conductivity and therefore, cathode reaction is limited to triple-phase boundary (TPB) area where LSM cathode, YSZ electrolyte and oxygen are in contact with each other (4). In order to improve the performance of LSM